Valence Bond Perturbation Theory. A Valence Bond Method That Incorporates Perturbation Theory†

Zhenhua Chen,‡ Jinshuai Song,‡ Sason Shaik,§ Philippe C. Hiberty,|| and Wei Wu*,‡

The State Key Laboratory of Physical Chemistry of Solid Surfaces and College of Chemistry and Chemical Engineering, Xiamen University, Xiamen, Fujian 361005, China, Institute of Chemistry and The Lise Meitner-Minerva Center for Computational Quantum Chemistry, The Hebrew University, Jerusalem, 91904, Israel, and Laboratoire de Chimie Physique, Groupe de Chimie Théorique, CNRS UMR 8000, Université de Paris-Sud, 91405 Orsay Cédex, France

Received: April 1, 2009; Revised Manuscript Received: June 1, 2009

A post-VBSCF method, called valence bond second-order perturbation theory (VBPT2), is developed in this paper and is shown to be (i) economical and (ii) at par with more sophisticated VB and MO-based methods. The VBPT2 method starts with VBSCF using a minimal structure set. Subsequently, the Møller−Plesset (MP) partition of the zeroth-order Hamiltonian is obtained by introducing a generalized Fock matrix constructed from the VBSCF density matrix. The first-order wave function is expressed in terms of singly and doubly excited VB structures, which are generated by replacing occupied orbitals by virtual orbitals, the latter being defined as orthogonal to the occupied orbitals. The VBPT2 method retains the simplicity of a VB presentation by condensing contributions from the excited structures into the minimal number of fundamental structures that are involved in the VBSCF calculation. The method is tested by calculating the bond energies of H_2, F_2, N_2, O_2, the barrier of identity hydrogen abstraction reaction, the atomization energy and a potential energy curve for the water molecule and the structural weights and covalent−ionic resonance energy of F_2. It is shown that the VBPT2 method gives results in good agreement with those of the VBCI method and molecular-orbital based methods such as MRPT and MRCI at the same truncation levels. However, the computational effort is greatly reduced, compared to that of VBCI. Future potential directions for the development of the VBPT2 method are outlined.

1. Introduction

Molecular orbital (MO) theory, which is based on delocalized molecular orbitals, is nowadays the main computational tool in contemporary quantum chemistry. Nevertheless, valence bond (VB) theory, which is based on localized atomic orbitals (AOs) or hybrid atomic orbitals (HAOs), remains as a widespread conceptual matrix for many chemists.[1] VB methods[2−8] generally require expensive computational effort, owing to the use of nonorthogonal AOs, while their accuracies are not always satisfactory. As such, the stumbling block for the development of VB theory has always been its lack of efficient computational approaches that would possess both quantitative accuracy and acceptable computational cost.

The classical VB method uses covalent and ionic structures based on unoptimized AOs, and thus is extremely poor. As one of the modern VB methods, the valence bond self-consistent field (VBSCF) method[3] optimizes VB orbitals and structural coefficients simultaneously, and gets improvement in accuracy. Mathematically, the VBSCF method is equivalent to the CASSCF method, for a given dimension of the orbital space and if all the VB structures with delocalized orbitals are considered. However, usually VB methods employ only a few structures that are essential to describe the system of interest, whereas CASSCF uses the complete set of configurations within the active space. In accord, the VBSCF results are often less accurate than those of CASSCF. At the same time, both CASSCF and VBSCF methods include some degree of static electron correlation, but completely lack dynamic correlation, which is very important for obtaining accurate bonding energies or energy gaps between electronic states. Other VB methods include generalized VB (GVB)[5] and spin coupled VB (SCVB)[6] methods, which use "overlap-enhanced orbitals" (OEOs) that are fairly localized on a given center but contain small tails on other centers.

A VB method which incorporates dynamic correlation is the breathing orbital VB (BOVB) method.[7] This method allows different VB structures to have their own orbital sets during orbital optimization procedure. Thus, the orbitals adapt themselves to the instantaneous field of each VB structure, rather than to the mean field of all the structures, as is the case in VBSCF. This additional degree of freedom in BOVB introduces dynamic correlation, and thereby improves considerably the accuracy of the results.

A few years ago, some of us[8] introduced a VB method, called configuration interaction valence bond (VBCI), which accounts for dynamic correlation, using a CI technique. The method uses optimized VB orbitals from a VBSCF calculation as occupied VB orbitals and subsequently constructs properly localized virtual VB orbitals that are localized and orthogonal to the occupied orbitals of the same fragments. These virtual VB orbitals are used, in turn, to generate excited VB structures by replacing occupied VB orbitals by their corresponding virtual orbitals. In this manner, the extensive VBCI wave function is condensed into a minimal set of fundamental structures that are

‡ Xiamen University.
§ The Hebrew University.
|| Université de Paris-Sud.
† Part of the "Walter Thiel Festschrift".
* To whom correspondence should be addressed. E-mail: weiwu@xmu.edu.cn. Fax: (86)592-2183047.

10.1021/jp903011j CCC: $40.75
Published on Web 07/01/2009

used in the VBSCF calculation, and thus VBCI retains the simplicity of a VBSCF presentation.

While our recent VBCI applications[9] showed that the accuracy of VBCI applications is always satisfactory, still the method is computationally demanding. The stumbling blocks in a VBCI calculation are (i) the construction of the Hamiltonian and overlap matrices, which requires expensive effort due to the use of nonorthogonal AOs; and (ii) the solution of the general secular equation, where the overlap matrix is not unity. Both of these steps are time-consuming, compared to the MO-based CI methods, in which the Hamiltonian matrix is sparse and easily computed by using Condon−Slater rules. Thus, an economical VB method that contains both static and dynamic correlation effect and is at par with MO-based methods is still a targeted goal.

Perturbation theory is known to be an economical approach for electronic correlation, and is widely applied in MO-based methods, like the single-reference-based MP2 method, or multireference-based methods, such as CASPT2[10] and MBPT2.[10−13] In the VB framework, perturbation theory is also used in the GVB[14,15] and SCVB methods.[16] In this paper, we will present a VB method called valence bond second order perturbation theory (VBPT2), which incorporates a perturbative treatment of excited VB structures. In this method, the MP partition of the zeroth-order Hamiltonian is defined by introducing a generalized Fock matrix that is constructed from the VBSCF density matrix. The first-order wave function is expressed in terms of singly and doubly excited VB structures, which are generated by replacing occupied orbitals by virtual orbitals that are defined so as to be orthogonal to the occupied ones. As shall be demonstrated, the VBPT2 method is much more efficient than the VBCI method, while its accuracy is satisfactory.

2. Theory and Methodology

2.1. Valence Bond Self-Consistent Field (VBSCF) Method. In the VBSCF method, a many-electron wave function is expressed in terms of a set of VB functions, called fundamental structures, which are essential to the description for the particular chemical problem,

$$\Psi^{\mathrm{VBSCF}} = \sum_K C_K^{(0)} \Phi_K \tag{1}$$

where Φ_K may be either a spin-coupled form, called Heitler−London−Slater−Pauling (HLSP) function, or a tableau function,[4] if the spin-free form of quantum chemistry[17] is used. Traditionally, a HLSP function is expressed as a linear combination of Slater determinants, which are built upon AOs, while a spin-free VB function is defined by using the projection operator of the symmetric group. The procedure for evaluating the Hamiltonian and overlap matrices is described in detail elsewhere[4,18] and will not be addressed in this paper.

During the VBSCF procedure, the structure coefficients $C_K^{(0)}$ and VB orbitals ϕ_m are optimized simultaneously by minimizing the total energy E^{SCF}, which is determined by solving the usual secular equation,

$$\mathbf{H}^{\mathrm{SCF}}\mathbf{C}^{(0)} = E^{\mathrm{SCF}}\mathbf{M}^{\mathrm{SCF}}\mathbf{C}^{(0)} \tag{2}$$

where $\mathbf{H}^{\mathrm{SCF}}$ and $\mathbf{M}^{\mathrm{SCF}}$ are the Hamiltonian and overlap matrices in the basis of VBSCF functions, defined as in eq 3:

$$H_{KL}^{\mathrm{SCF}} = \langle \Phi_K | H | \Phi_L \rangle \quad \text{and} \quad M_{KL}^{\mathrm{SCF}} = \langle \Phi_K | \Phi_L \rangle \tag{3}$$

The VBSCF structure weights can be evaluated by the Coulson−Chirgwin formula, eq 4:

$$W_K^{\mathrm{SCF}} = \sum_L C_K^{(0)} M_{KL}^{\mathrm{SCF}} C_L^{(0)} \tag{4}$$

The form of VB orbitals depends on the requirement of the particular application; they may be localized, delocalized, or semilocalized. In the process of orbital optimization, the evaluation of energy gradients is the most time-consuming step. One widely used method is the super-CI method,[19] which is based on the generalized Brillouin theorem.[20] Another strategy is based on a numerical algorithm.[18a] Very recently, we presented an algorithm[18b] for evaluating the energy gradients by computing the derivative of the density with respect to the coefficients of basis functions.

In the VBPT2 method, the VBSCF wave function is defined as the reference wave function from which excitations are generated and treated by perturbation, in the same way as the CASSCF wave function serves as a reference in the CASPT2 method.[10]

2.2. Block-Orthogonalized Orbitals and Excited VB Structures. Throughout the present paper, we will distinguish the various orbitals according to their occupancies in the reference VBSCF wave function. The inactive orbitals are those that are always doubly occupied (indices $i, j, k, l, \ldots$), the active orbitals are the remaining occupied orbitals, with variable occupancies (indices $u, v, w, \ldots$), and the virtual orbitals are always unoccupied in the VBSCF reference (indices $a, b,$ c, . . .). The indices m and n denote any occupied orbitals (inactive + active), while the indices $p, q, r, s, \ldots$ denote any orbitals. For the VB structures, the indices $K, L, \ldots$ will denote the structures involved in the VBSCF reference, whereas $R, S, \ldots$ will refer to excited VB structures.

In the traditional VBSCF method, only occupied orbitals are optimized in the calculation and virtual orbitals are not defined. On the other hand, virtual orbitals are required if one wants to perform a post-VBSCF calculation involving excited VB structures. However, to create physically clear excited structures, the virtual orbitals must be strictly localized on fragments, while virtual orbitals belonging to the same fragment must maintain orthogonality mutually, as was previously done in the VBCI method.[8] In the VBPT2 method, the orthogonality constraint is generalized, for the sake of computational efficiency, by defining the virtual orbitals as orthogonal to all occupied orbitals over the whole molecule. To this end, a Schmidt orthogonalization is performed for basis functions as follows:

$$\chi_\mu{}' = \chi_\mu - \sum_m (\mathbf{ST}(\mathbf{T}^+\mathbf{ST})^{-1})_{\mu m}\phi_m \tag{5}$$

where χ_μ is a basis function, $\mathbf{S}$ is the overlap matrix of basis functions, and $\mathbf{T}$ is the coefficient matrix of VBSCF orbitals. This generates a set of virtual orbitals, but this set is overcomplete. The linearly independent virtual orbitals are determined by diagonalizing the overlap matrix of the new basis functions $\{\chi_\mu'\}$ and keeping the eigenvectors which share nonzero eigenvalues. In general, virtual orbitals are not strictly localized anymore, but their shapes are localized mainly on a fragment with orthogonalization tails over other fragments.

In brief, orbitals are partitioned into three groups, inactive, active, and virtual orbitals, such that (i) the inactive and virtual orbitals are orthogonal and (ii) the active orbitals are kept in

the VB spirit as mutually nonorthogonal, but are orthogonal to the inactive and virtual ones by a Schmidt orthogonalization. Such a definition of the orbitals keeps the VBSCF energy invariant, while the orthogonalization between orbital groups ensures the efficiency of VBPT2 method.

During the PT2 procedure, the excited VB structures are generated from the VBSCF structures by replacing occupied orbitals by virtual orbitals. It may happen that excited structures that are generated from different fundamental structures are linearly dependent. A checking procedure is performed by diagonalizing the overlap matrix of excited structures, where the eigenfunctions corresponding to the zero-eigenvalue are removed. The excitation levels are designated as single (S), double (D), and so on, where (S) involves one orbital replacement, while (D) involves two orbital replacements. The space containing all singly and doubly excited structures is designated as V^{SD}.

2.3. The Zeroth-Order Hamiltonian. In a similar fashion to MO-based multireference perturbation theory, we define a one-electron Fock operator,

$$\hat{f}(i) = \hat{h}(i) + \sum_{m,n} D_{mn}^{SCF}\left(\hat{J}_{mn}(i) - \frac{1}{2}\hat{K}_{mn}(i)\right) \tag{6}$$

where $\hat{J}_{mn}$ and $\hat{K}_{mn}$ are Coulomb and exchange operators, respectively, and D_{mn}^{SCF} is an element of the VBSCF density matrix. The matrix elements of the Fock operator are written as

$$f_{pq} = h_{pq} + \sum_{m,n} D_{mn}^{SCF}\left[(pq|mn) - \frac{1}{2}(pm|qn)\right] \tag{7}$$

The Fock matrix **f** in eq 7 may be transformed into a simple form by diagonalizing the blocks of the inactive and virtual orbital spaces, because the linear transformation of orbitals within the inactive and virtual spaces does not change the VBSCF wave function. With the transformed inactive and virtual orbitals, the Fock operator $\hat{f}$ is diagonal for both of inactive and virtual blocks, i.e.,

$$f_{ij} = \delta_{ij}\varepsilon_i \quad \text{and} \quad f_{ab} = \delta_{ab}\varepsilon_a \tag{8}$$

Furthermore, the Fock matrix elements between different sets are neglected, which is also optional in the CASPT2 method, namely, CASPT2D.

Using the Fock operator defined in eq 6, the zeroth-order Hamiltonian is defined as

$$\hat{H}_0 = \hat{P}_0\hat{F}\hat{P}_0 + \hat{P}_K\hat{F}\hat{P}_K + \hat{P}_{SD}\hat{F}\hat{P}_{SD} + \ldots \tag{9}$$

where $\hat{F} = \sum_i \hat{f}(i)$, $\hat{P}_0 = |0\rangle\langle 0|$ is a projector onto the VBSCF space, $\hat{P}_K$ is a projector onto the complementary space to the VBSCF wave function, and $\hat{P}_{SD}$ is a projector associated with singly and doubly excited structures from the reference wave function. If the VBSCF wave function is taken as a Slater determinant of doubly occupied inactive orbitals, the zeroth-order Hamiltonian reduces to the Hartree−Fock-based MP2 theory.

It may be shown that the VBSCF wave function is an eigenfunction of the zeroth-order Hamiltonian $\hat{H}_0$ with eigenvalue

$$E^{(0)} = \langle 0|\hat{F}|0\rangle \tag{10}$$

2.4. The First-Order Wave Function and the Second-Order Energy. In multireference second-order perturbation theory, the wave function is written as the sum of the zeroth-order and the first-order wave functions,

$$|\Psi\rangle = |\Psi^{(0)}\rangle + |\Psi^{(1)}\rangle \tag{11}$$

Here, the VBSCF wave function is taken as the reference zeroth-order wave function for further perturbative treatment:

$$|\Psi^{(0)}\rangle = |\Psi^{SCF}\rangle = \sum_K C_K^{(0)}|\Phi_K\rangle \tag{12}$$

Since higher-order excitations do not contribute to the first-order interacting space, the first-order wave function is written as a linear combination of the singly and doubly excited structures,

$$\Psi^{(1)} = \sum_{R\in V^{SD}} C_R^{(1)}|\Phi_R\rangle \tag{13}$$

Due to the orthogonality between the occupied and virtual orbitals, structures belonging to the V^{SD} space are orthogonal to the VBSCF space V^{SCF},

$$\langle\Psi^{(0)}|\Psi^{(1)}\rangle = 0 \tag{14}$$

Then the intermediate normalization condition holds,

$$\langle\Psi^{(0)}|\Psi\rangle = 1 \tag{15}$$

According to the Rayleigh−Schrödinger perturbation theory, the expansion coefficients of first-order wave function and the second-order energy are written respectively as

$$\mathbf{C}^{(1)} = (\mathbf{H}_0^{11} - E^{(0)}\mathbf{M}^{11})^{-1}\mathbf{H}^{10}\mathbf{C}^{(0)} \tag{16}$$

$$E^{(2)} = \mathbf{C}^{(0)}\mathbf{H}^{01}(\mathbf{H}_0^{11} - E^{(0)}\mathbf{M}^{11})^{-1}\mathbf{H}^{10}\mathbf{C}^{(0)} \tag{17}$$

where $\mathbf{C}^{(0)}$ and $\mathbf{C}^{(1)}$ are the coefficient column matrices of the VBSCF wave function, eq 12, and the first-order wave functions, eq 16, respectively, $E^{(0)}$ is the zeroth-order energy, and matrices $\mathbf{H}_0^{11}$, $\mathbf{H}^{01}$, $\mathbf{H}^{10}$, and $\mathbf{M}^{11}$ are respectively defined as

$$(H_0^{11})_{RS} = \langle\Phi_R|\hat{H}_0|\Phi_S\rangle \tag{18}$$

$$(H^{01})_{KR} = \langle\Phi_K|\hat{H}|\Phi_R\rangle, \quad (H^{10})_{RK} = \langle\Phi_R|\hat{H}|\Phi_K\rangle \tag{19}$$

$$(M^{11})_{RS} = \langle\Phi_R|\Phi_S\rangle \tag{20}$$

It is obvious that the most time-consuming part in solving eqs 16 and 17 is the inversion of the matrix $(\mathbf{H}_0^{11} - E^{(0)}\mathbf{M}^{11})$, which is block-diagonal, owing to the orthogonality constraints

that are applied to the different orbital sets and the block-diagonal form of the Fock matrix. Furthermore, any element of this matrix between two excited structures differing by one inactive or virtual orbital is zero.

2.5. The Structural Weights in the VBPT2 Method. One of the most important advantages of modern VB theory is its ability to provide chemical insight with a compact wave function.[1a] The VBSCF wave function is written as a linear combination of a small set of fundamental structures, and this compactness makes the wave function particularly insightful. In the VBPT2 method, the VBSCF wave function is augmented by the first-order wave function, which usually involves a large number of excited structures. To keep the VBPT2 wave function as compact as in the VBSCF method, it is necessary to partition the first-order wave function into the fundamental structures of the reference VBSCF function. To this end, a PT function Φ_K^{PT}associated with the fundamental structure Φ_K is defined as

$$\Phi_K^{\mathrm{PT}} = N_K(\Phi_K + \sum_R X_{RK}\Phi_R) \tag{21}$$

where the coefficient matrix $\mathbf{X}$ is defined as

$$\mathbf{X} = (\mathbf{H}_0^{11} - E^{(0)}\mathbf{M}^{11})^{-1}\mathbf{H}^{10} \tag{22}$$

and the normalization factor is given as

$$N_K = (1 + \sum_{R,S} X_{RK}M_{RS}^{11}X_{SK})^{-1/2} \tag{23}$$

From eq 21, it can be seen that the first-order wave function is partitioned referred to the fundamental structure Φ_K, i.e.,

$$C_R^{(1)} = \sum_K X_{RK}C_K^{(0)} \tag{24}$$

Thus, the wave function in VBPT2 can be written as

$$\Psi^{\mathrm{VBPT}} = \sum_K C_K^{\mathrm{PT}}\Phi_K^{\mathrm{PT}} \tag{25}$$

where

$$C_K^{\mathrm{PT}} = C_K^{(0)}\left[\frac{1 + \sum_{R,S} X_{RK}M_{RS}^{11}X_{SK}}{1 + \sum_{R,S}\sum_{L,L'} C_L^{(0)}X_{RL}M_{RS}^{11}X_{SL'}C_{L'}^{(0)}}\right]^{1/2} \tag{26}$$

Equation 25 shows that the VBPT2 method enables one to represent the VBPT2 wave function in a compact form. Therefore, the weights of the fundamental structures with perturbation correction can be defined as

$$W_K^{\mathrm{PT}} = \sum_L C_K^{\mathrm{PT}}M_{KL}^{\mathrm{PT}}C_L^{\mathrm{PT}} \tag{27}$$

where M_{KL}^{PT} is the overlap matrix of the fundamental structures, defined as

$$M_{KL}^{\mathrm{PT}} = \langle\Phi_K^{\mathrm{PT}}|\Phi_L^{\mathrm{PT}}\rangle = N_K N_L(M_{KL}^{\mathrm{SCF}} + \sum_{R,S} X_{RK}M_{\mathrm{RS}}^{11}X_{SL}) \tag{28}$$

Similarly, the second-order energy can be written as

$$E^{(2)} = \sum_{K,L} C_K^{(0)}E_{KL}^{(2)}C_L^{(0)} \tag{29}$$

where

$$E_{KL}^{(2)} = \sum_R H_{KR}^{01}X_{RL} \tag{30}$$

$E_{KL}^{(2)}$ is the second-order correction to the Hamiltonian matrix element H_{KL}^{SCF},

$$H_{KL}^{\mathrm{PT}} = H_{KL}^{\mathrm{SCF}} + E_{KL}^{(2)} \tag{31}$$

Therefore, the extensive VBPT2 wave function is condensed into a minimal set of fundamental VB structures that are all dressed with dynamic correlation.

2.6. Calculation of Diabatic States. Although no unique definition actually exists, a diabatic state is generally defined as a wave function that keeps a constant physical content throughout a potential surface. Such states are extremely useful in molecular dynamics or in reactivity models,[21] and are well represented by a unique VB structure or a restricted combination of VB structures. It is therefore essential that the VBPT2 method be able to calculate the energies of diabatic states in good agreement with the VBCISD results. Diabatic energies can be obtained in two ways: either by projection from the wave function of the ground state or, more simply, by directly calculating the energy of the VB structure or group of VB structures that represent the diabatic state. It is this latter option that has been chosen in this work.

3. Applications: Results and Discussion

In order to test the performance of the VBPT2 method as compared to VBCISD and other computational methods, some bond dissociation energies, reaction barrier, atomization energy, structural weights and resonance energies are presented in this section. All the orbitals used for the VBSCF calculations are strictly localized on their own atoms. The calculations were performed with the Xiamen valence bond (XMVB) package. To obtain basis set integrals and nuclear repulsion energy, preliminary ROHF calculations are carried out using the Gaussian 03 package.[22]

3.1. The Dihydrogen Molecule. Dihydrogen played an extremely important role in the early history of molecular quantum mechanics. In 1927 Heitler and London (HL) published their seminal paper[23] on the origins of the chemical bond in the H_2 molecule, using Heisenberg's resonance approach.[24] Since then, dihydrogen has been taken as a typical example for VB theory in textbooks. In this work, the standard aug-cc-pvTZ basis set is employed in the calculation, and three fundamental VB structures, one covalent and two ionic structures, as shown in Scheme 1, are used for the VBSCF calculations. The spectroscopic parameters r_e, ω_e and D_e are computed using three points with 0.05 a_0 separation fit to a second-degree polynomial in $1/R$ as that used by Bauschlicher and Langhoff. It should be

SCHEME 1: The VB Structure Set for H_2

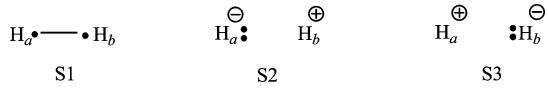

S1 S2 S3

TABLE 1: Some Calculated Spectroscopic Constants of H_2

method	r_e (a_0)	ω_e (cm^{-1})	D_e (eV)
FCI	1.405	4421	4.707
CASSCF[a]	1.427	4255	4.14
CASPT2N[a]	1.410	4407	4.57
VBSCF	1.429	4193	4.121
VBPT2	1.408	4376	4.609
VBCISD	1.405	4421	4.707

[a] Reference 10b, where the ANO(4s3p2d) basis set was used and orbitals $1\sigma_g$ and $1\sigma_u$ are taken as active orbitals.

noted that these three-point fits to the calculated potential are only accurate to within ~20 cm^{-1}.[14a]

Table 1 shows the spectroscopic constants of H_2 obtained by various VB methods, alongside MO-based results. It can be seen that the spectroscopic constants computed by the VBSCF method are in very good agreement with those of the CASSCF method. As expected, neither of them is quantitatively good, compared to the full CI results. On the other hand, the VBPT2 results are virtually identical to CASPT2 ones, and very close to the full CI results. Relative to the VBSCF level, VBPT2 reduces the errors in r_e, ω_e and D_e from 0.024 to 0.003 a_0, from 228 to 45 cm^{-1} and from 0.586 to 0.098 eV, respectively. As expected, the VBCISD results are exactly the same as those of FCI, as they are equivalent for a two-electron molecule.

3.2. Spectroscopic Constants of the Ground State of Dioxygen. As the second example, we study the bond-breaking process of a multiply bonded diatomic molecule, dioxygen, which has been studied recently with the VBCI method.[9b] Multiple bonds are generally difficult test cases for any method, for dynamic correlation is essential for getting quantitative accuracy. For the sake of comparison to the full CI results of Bauschlicher and Langhoff,[25] the same double-ζ plus polarization basis set (DZP) is used in the present work, and the two lowest-lying orbitals are kept as inactive core orbitals that remain doubly occupied in both the VBSCF and post-VBSCF wave functions. The spectroscopic parameters r_e, ω_e and D_e were fitted in the same way as in the calculation of the H_2 molecule.

In our previous study of the dioxygen molecule, based on the analysis of the electron pairing pattern, twelve fundamental VB structures were found necessary to represent the triplet ground state in a balanced way. These VB structures, shown in Scheme 2, describe the dioxygen molecule as displaying a σ bond and two three-electron π bonds, one in each π plane. In the present work, the VBPT2 calculations are performed at two levels of accuracy, differing by the choice of the VBSCF reference function. At the first level, the VBSCF reference, designated as VBSCF(12), involves the twelve fundamental structures of Scheme 2. At the second level, the VBSCF reference includes all 105 structures that can be generated by arranging six electrons in six atomic orbitals to form a triplet state. In this latter reference function, designated as VBSCF(105), the VB orbitals are taken from the VBSCF(12) calculation and not further optimized. The corresponding two post-VBSCF levels will be referred to as VBPT2(12) and VBPT2(105), respectively. The spectroscopic constants of O_2, as calculated by the various methods, are collected in Table 2.

As can be seen, the VBSCF(12) results are not quantitatively satisfactory, compared to the FCI results. The errors in r_e and

SCHEME 2: The VB Structure Set for O_2

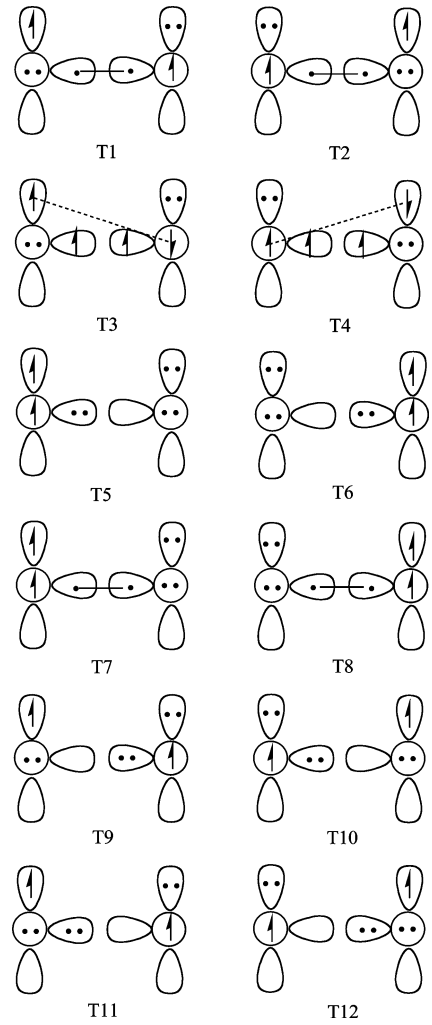

TABLE 2: Some Calculated Spectroscopic Constants for the Ground State of O_2

method	r_e (a_0)	ω_e (cm^{-1})	D_e (eV)
FCI[a]	2.318	1608	4.637
VBSCF(12)[b]	2.368	1580	2.999
VBPT2(12)[b]	2.333	1560	4.327
VBSCF(105)[c]	2.368	1581	3.045
VBPT2(105)[c]	2.324	1601	4.661
VBCISD(12)[b,d]	2.333	1594	4.154
VBCISD[e]	2.336	1545	4.77
CASSCF[f]	2.322	1566	3.678
CASPT2N[f]	2.317	1607	4.658

[a] Reference 25. [b] Twelve fundamental VB structures are used. [c] 105 fundamental structures are used, but the orbitals are optimized at the VBSCF(12) level. [d] Three orbital blocks, σ, π_x and π_y, are used. [e] Reference 9b, where the cc-pVTZ basis set is used. [f] Reference 10c.

D_e are 0.050 a_0 and 1.638 eV, respectively, and the VBSCF(105) level performs hardly better. On the other hand, the calculated frequencies are satisfactory at these levels, being close to the FCI value to within 28 cm^{-1}.

The results are considerably improved when perturbation corrections are applied. For the equilibrium distance r_e, the deviation relative to FCI reduces to 0.015 a_0 at the VBPT2(12) level, and to only 0.006 a_0 at the VBPT2(105) level. For the dissociation energy, the VBSCF(12) value which was much too low is increased by 1.328 eV at the VBPT(12) level, which is

TABLE 3: Deviation in Total Energies (hartree) from Full CI for O_2 in a DZP Basis as a Function of the O−O Distance (a_0)

method	2.25 a_0	2.30 a_0	2.35 a_0	100.0 a_0
FCI[a]	−149.87515	−149.87695	−149.87669	−149.70668
VBSCF(12)[b]	0.169718	0.167519	0.165512	0.105588
VBPT2(12)[b]	0.021598	0.021088	0.020528	0.009433
VBSCF(105)[c]	0.168036	0.16583	0.163819	0.105588
VBPT2(105)[c]	0.008849	0.008623	0.008404	0.009433
VBCISD(12)[b,d]	0.046259	0.045649	0.045076	0.027891
CASSCF[e]	0.14325	0.14317	0.14300	0.10788
CASPT2N[e]	0.00488	0.00482	0.00476	0.00560

[a] The total energy is given, ref 25. [b] 12 fundamental VB structures are used. [c] 105 fundamental structures are used, but VB orbitals are optimized at the VBSCF(12) level. [d] Three orbital blocks, σ, π_x, π_y, are used in the VBCI calculation. [e] Reference 10c.

slightly better than VBCISD (1.155 eV), but still deviates by 0.310 eV from the FCI value. This remaining error is completely corrected at the VBPT2(105) level, which provides a D_e value within 0.024 eV of the FCI result, and close to the CASPT2N value. It is worthwhile to mention that VBPT2(105) uses only a small structure set (12 structures) for orbital optimization, and the result is that the computational cost in VBPT2(105) is not much more expensive than in VBPT2(12).

The frequency values ω_e, which are already quite accurate at the VBSCF levels, are not improved at the VBPT(12) level, but come even closer to the FCI value at the VBCISD and VBPT2(105) levels, with a remaining deviation of only 7 cm^{-1} in this latter case.

The total energies of O_2 as calculated by various methods are collected in Table 3. Unlike the MO-based MRCI method, the total energy of the VBPT2 is lower than its corresponding VBCISD. This is because the VBCI method includes only excited structures whose electronic pairing patterns and charge distributions are the same as the VBSCF structures. For the 12-structure based calculation, the biggest deviation from FCI occurs near 2.25 a_0, and amounts to 168 mhartree for VBSCF and 22 mhartree for VBPT2(12). The deviation of VBPT2(105) is about 9 mhartree at 2.25 a_0, and remains remarkably constant at the different geometries. The deviations of VBPT2(105) are very close to those of CASPT2N.

3.3. Spectroscopic Constants of the Ground State of Dinitrogen. As the third example, we study another classical test case, the bond breaking process of the dinitrogen molecule, which displays a triple bond in its singlet ground state. As has been done in the dioxygen case, our results are compared with the full CI results of Bauschlicher and Langhoff,[25] and to that aim we have used the same double-ζ polarization (DZP) basis as these authors, and kept the two lowest-lying orbitals as inactive core orbitals that remain doubly occupied at all levels. The spectroscopic parameters r_e, ω_e and D_e were fitted in the same way as in the calculation of the H_2 molecule.

The VB structures that form the fundamental set for N_2 are chosen as follows. First a set of covalent structures is generated. This set includes the main covalent structure, S1, displaying one σ and two π bonds, complemented with four VB structures, S2−S5, so as to form a complete and linearly independent set according to Rumer's method.[26] Then a set of monoionic structures, S6−S11, is generated from S1 by turning each covalent bond into an ionic bond, alternatively. Finally six dionic structures are generated, S12−S17, chosen so that each nitrogen atom remains neutral in the VB structure, therefore eliminating diionic structures displaying doubly charged atoms. The 17 selected VB structures are shown in Scheme 3. As in the dioxygen calculation above, two levels are used. The first level, designated as VBSCF(17), uses the 17 structures of Scheme 3 for the reference VBSCF and the subsequent PT2 calculation, called VBPT2(17). The second level uses the complete set of 175 VB structures that can be generated for a 6-orbital 6-electron singlet state, leading to the VBSCF(175) and VBPT2(175) wave functions. As in the preceding case, the orbitals optimized in the small set calculation are used indifferently at the two VBSCF levels as well as the corresponding VBPT2 levels. The

SCHEME 3: The VB Structure Set for N_2

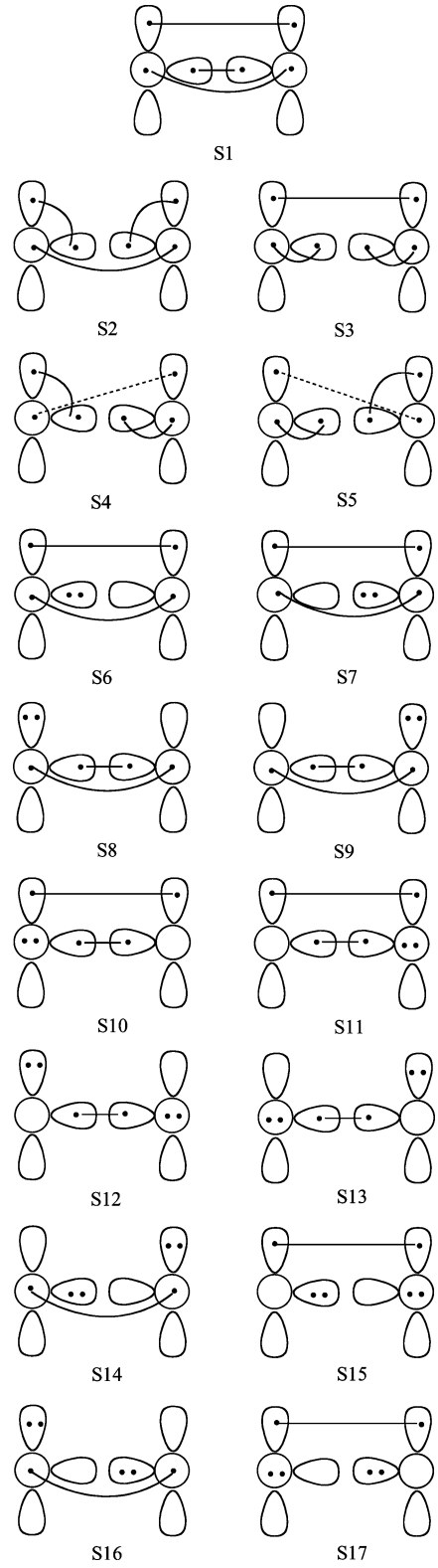

TABLE 4: Some Calculated Spectroscopic Constants for the Ground State of N_2

method	r_e (a_0)	ω_e (cm^{-1})	D_e (eV)
FCI[a]	2.123	2341	8.748
VBSCF(17)[b]	2.109	2388	8.086
VBPT2(17)[b]	2.115	2373	8.421
VBSCF(175)[c]	2.114	2364	8.190
VBPT2(175)[c]	2.120	2344	8.573
VBCISD(17)[b]	2.121	2330	8.651
CASSCF[d]	2.119	2337	8.333
CASPT2N[d]	2.122	2342	8.621

[a] Reference 25. [b] Seventeen fundamental VB structures are used. [c] 175 fundamental VB structures are used, but the VB orbitals are optimized at the VBSCF(17) level. [d] Reference 10c.

SCHEME 4: The VB Structure Set for F_2

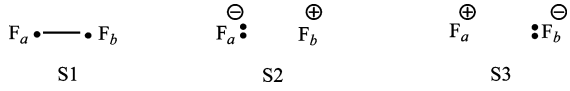

spectroscopic constants of the ground state of N_2, as calculated by various methods, are collected in Table 4.

It can be seen that the spectroscopic parameters computed at the VBSCF(17) and VBSCF(175) levels are in good agreement with each others, showing the adequacy of the 17-structure set. Hence VBSCF(17) provides a good starting point for a perturbation calculation to improve the accuracy of calculations. The perturbation correction, VBPT2(17), reduced the error in r_e from 0.014 a_0 in VBSCF(17) to 0.008 a_0, while for VBPT2(175), the error is further reduced to 0.003 a_0, which is virtually identical to that of CASPT2N. For the bond dissociation energies the VBSCF values are less erroneous than in the dioxygen case, with errors of 0.662 and 0.558 eV at the VBSCF(17) and VBSCF(175) levels, respectively. VBPT2(17) recovers 0.335 eV of the bond energy, still with a deviation of 0.327 eV relative to the FCI value. The VBPT2(175) level further improves the value of bonding energy, with a remaining absolute error of 0.175 eV (i.e., 2% in relative error), close to the CASPT2 and VBCISD values. For the calculated frequencies, VBPT2(17) does not get much improvement over the VBSCF(17) calculation, while the VBPT2(175) value matches the FCI one very well with a deviation of only 3 cm^{-1}.

3.4. The Difluorine Molecule. The difluorine molecule is known to be a difficult test case for any computational method since the molecule is found to be unbound at the Hartree−Fock limit. As is well-known, the Hartree−Fock failure is due to its overestimation of the weights of the ionic components, particularly high in energy in this molecule. Therefore quantitatively accurate bonding energies require the VB method to provide a balanced description of ionic and covalent structures, in a manner that accounts for both static and dynamic electronic correlation. The F_2 molecule will therefore be used as a test to examine the abilities of the various methods to reproduce the spectroscopic parameters, but also the weights of the covalent and ionic structures and the energies of the diabatic covalent structures relative to the ground state. In this work, all the 18 electrons are involved in the VB calculations, with the two lowest-lying orbitals (actually the core orbitals) being kept as doubly occupied inactive orbitals. The structure set for the initial VBSCF calculation is shown in Scheme 4, using strictly localized hybrid atomic orbitals (HAOs), and a correlation-consistent basis set of triple-ζ plus polarization quality, cc-pVTZ basis set. The r_e and D_e value of the VBSCF and VBPT2 methods are obtained using a fit of three points with 0.03 Å separation to a second-degree polynomial in $1/R$.

TABLE 5: Spectroscopic Constants for F_2

method	r_e (a_0)	ω_e (cm^{-1})	D_e (kcal/mol)
VBSCF	2.784	552.7	10.05
VBPT2	2.683	905.3	35.72
VBCISD	2.689	886.8	35.35
L-BOVB	2.700	892.7	33.32
CASSCF[a]	2.755	803.1	19.62
CASPT2[a]	2.691	899.1	35.19
MRCI[a]	2.680	889.5	32.81
expt[b]	2.668	917	38.0

[a] The MOLPRO package is used for the CASSCF(2,2), CASPT2 and MRCI calculations.[32] [b] Reference 29.

TABLE 6: Weights of the VB Structures and Resonance Energy (RE) of F_2, at an F−F Distance of 2.70 a_0

method	W_{cov}	W_{ion1}/W_{ion2}	RE (kcal/mol)
VBSCF	0.785	0.108	46.28
L-BOVB	0.695	0.152	71.46
VBCISD	0.730	0.135	60.68
VBPT2	0.778	0.111	60.02

Table 5 displays the bond dissociation energies as computed by various VB and MO methods. As expected, the VBSCF and CASSCF levels, which lack dynamic correlation, provide too long equilibrium distances, too low frequencies, and very poor dissociation energies. While no full CI calculation has been reported, to our knowledge, for this molecule, the CASPT2 and MRCI calculations both provide equilibrium bond lengths and frequencies in reasonable agreement with experiment. On the other hand, these methods yield dissociation energies on the low side, 33−35 kcal/mol, of the experimental value of 38 kcal/mol. However these differences are normal as the F_2 molecule is known to require very large basis sets for experimental properties to be accurately reproduced. Thus, the MRCI and CASPT2 spectroscopic constants are probably very close to the values that would arise from full CI. As for the VBPT2 level, it provides bonding distance, frequency and dissociation energies in very good agreement with VBCISD, both methods matching the CASPT2 values very well with differences smaller than 1 kcal/mol for the bonding energy. The L-BOVB level provides a slightly smaller D_e and longer r_e, however it must be remembered that the BOVB method has several levels of sophistication, L-BOVB being the lowest one.

Let us now turn to the diabatic states of the F_2 molecule, i.e. the purely covalent (S1 in Scheme 4) and purely ionic VB structures (S2 and S3). These structures are unambiguously defined in the BOVB method and also in VBCISD, in which all the orbitals, occupied as well as virtual, are strictly localized. On the other hand, the purely covalent or ionic nature of the diabatic states is less strictly established in the VBPT2 method, as the virtual orbitals are not strictly localized (vide supra). Therefore, it is important to check that the VBPT2 method and its close analogue VBCISD provide values that do not differ too much from each others for the weights and energies of the diabatic structures.

Table 6 shows the weights of the covalent and ionic structures for F_2 ($R_{FF} = 2.70$ a_0). It can be seen that the weights for various methods are in good agreement for all the methods. The BOVB and VBCISD values for the weight of the covalent structure are in fair agreement with each others, but not quite equal, indicating a slight influence of the correlation of inactive electrons (not included in BOVB) on the structural weights. This latter effect is present in both VBCISD and VBPT2 methods, which nevertheless provide slightly different weights, a probable consequence of the nonperfect localization of virtual orbitals

in the latter method. However the differences are small and do not matter much for this quantity whose definition is only approximate and which is not an observable property.

Table 6 also shows the resonance energy (RE) arising from the mixing of covalent and ionic structures for F_2 ($R_{FF} = 2.70$ a_0), in other words the energy of the covalent structure alone relative to the ground state. In previous studies,[27] it has always been found that the VBCISD-calculated values for REs are systematically smaller than the BOVB-calculated ones. Which one of the methods give "better" REs is not important for an isolated case, since all the methods give large REs for this molecule, significantly larger than the corresponding BDE value. On the other hand, it is important that VBPT2 and VBCISD give similar results, since these two methods closely resemble each other as far as electron correlation is considered. Table 6 shows that this is indeed the case, as both methods provide about the same RE values in the range 60−61 kcal/mol. These results show that the VBPT2 method is able to provide not only accurate quantitative results for the ground state, but also important VB information for the diabatic states, that are essential to VB theory.

3.5. The H_2O Molecule. Another classical test for a novel method is the calculation of a complete potential energy curve (PEC). The symmetric stretching of the water molecule has often been used for that purpose.[28] Olsen and co-workers have presented a FCI calculation of the corresponding PEC,[28] using a basis set of valence double-ζ plus polarization quality (VDZP). For the sake of comparison, the same PEC is calculated in this work by the VBSCF and VBPT2 methods using the same basis set and geometries as in the reference calculation of Olsen and co-workers. The calculations are carried out using C_{2v} symmetry, where the water molecule is in the *yz* plane and the *z* axis is taken as the C_2 axis. The HOH bond angle is fixed as 110.6°. The active orbitals are those involved in the O−H bonds, namely the 1s orbitals of the hydrogen atoms and two hybrid atomic orbitals of oxygen, approximately of sp^3 type, and pointing to the hydrogen atoms. The remaining orbitals, i.e. the 1s core and the two lone pairs of oxygen, are doubly occupied inactive orbitals. The VBSCF calculation involves all the 20 VB structures that constitute a full VB space for a system of four electrons in four active orbitals (Scheme 5). Table 7 shows the total energy of the water molecule at various OH bond distances with different methods. Of course, what matters for judging the quality of the various methods is not the absolute energy by itself, but rather the constancy of the energy difference with the FCI values along the PEC. As can be seen, the VBSCF performance is rather poor in that respect, as its energy difference with FCI varies from 186 mhartree at the equilibrium geometry (R_e) to only 125 mhartree at $3*R_e$. The CASSCF method, despite a much larger number of configurations in the active space, performs hardly better. On the other hand, the CASPT2 PEC is fairly satisfactory, with energy differences with the FCI energies varying by only 5 mhartree, meaning that both levels of calculations yield PECs of rather similar shapes.

The VBPT2 calculations have been performed at two levels. At the first level, referred to as VBPT2(occ), only excitations from the occupied orbitals to virtual ones are involved. At the second level, VBPT2(all), the excitations form inactive orbitals to active ones are also included. While VBPT2(occ) performs slightly better than CASPT2 with deviations from FCI remaining fairly constant within 4 mhartree, from R_e all the way to $8*R_e$, the VBPT2(all) performs even better, yielding a PEC virtually parallel to the FCI one, with quasi-constant energy deviations, within 1 mhartree.

SCHEME 5: The VB Structure Set for H_2O

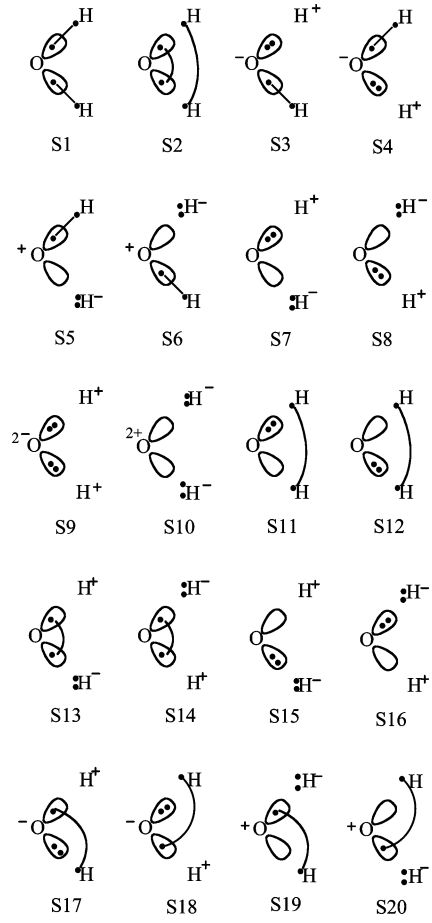

Table 8 collects the atomization energy of the water molecule as computed by the various methods. As expected from the above discussion, the VBSCF and CASSCF results are rather poor, with errors ranging from 29 to 39 kcal/mol, while CASPT2 and VBPT2 values, especially VBPT2(all), are in excellent agreement with the FCI value.

3.6. The H_3 Reaction Barrier. The identity hydrogen transfer, eq 32,

$$H{-}H + H^{\cdot} \rightarrow H^{\cdot} + H{-}H \qquad (32)$$

is the simplest reaction that describes bond exchange. As such, the accurate calculation of its barrier in the 1970s constituted a landmark achievement of quantum chemistry and specifically of MO-based methods that include electron correlation.[30] In a previous work,[9a] we demonstrated that the barrier could be very well reproduced at the BOVB and VBCISD levels in a standard basis set of moderate size, aug-cc-pVTZ. In this work, the barrier is calculated at the VBPT2 level, using the same basis set and the geometries of the transition state (TS) and reactants taken from our previous VBCISD/aug-cc-pVTZ calculations.[9a]

Eight VB structures, shown in Scheme 6, are necessary and sufficient to describe the electronic structure of $H_3^{\cdot}$. The VBPT2 results are displayed in Table 9, together with some calculated barriers at other VB levels, for comparison. The importance of dynamic correlation is demonstrated by the poor result of the VBSCF level, which provides much too high a barrier. On the other hand, all the VB levels that include dynamic correlation provide barriers in good agreement with the reference CCSD(T) value in the same basis set. In particular, the VBPT2 value of

TABLE 7: Deviation in Total Energies (hartree) from Full CI of H_2O as a Function of the Symmetric Stretching from the Equilibrium OH Distance R_e

method	R_e	1.5*R_e	2.0*R_e	2.5*R_e	3.0*R_e	8.0*R_e
FCI[a]	−76.241860	−76.072348	−75.951665	−75.917991	−75.911946	−75.91030
CASSCF(8,6)[b]	0.164025	0.150029	0.133568	0.126322	0.124715	
CASPT2[b]	0.012833	0.010819	0.008111	0.008033	0.008262	
VBSCF	0.185720	0.162571	0.137994	0.127189	0.124965	0.12423
VBPT2(occ)[c]	0.035294	0.037417	0.038052	0.039430	0.039699	0.039676
VBPT2(all)[d]	0.027409	0.026567	0.026782	0.028302	0.02866	0.028673

[a] The total energy is given.[28] [b] Reference 28. [c] Only excitations from occupied orbitals to virtual ones are included. [d] All excitations are included, involving excitations from inactive orbitals to active ones.

TABLE 8: Calculated Atomization Energy of H_2O

method	D_e (kcal/mol)[a]
FCI[b]	208.06
CASSCF[c]	179.6
CASPT2[c]	210.4
VBSCF	169.47
VBPT2(occ)[d]	210.81
VBPT2(all)[e]	208.85

[a] $D_e = E(R_e) - E(8*R_e)$. [b] Reference 28. [c] Reference 31. [d] Only excitations from occupied orbitals to virtual ones are included. [e] All excitations are included, involving excitations from inactive orbitals to active ones.

SCHEME 6: The VB Structure Set for H_3

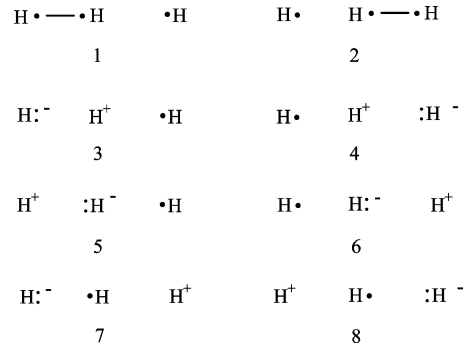

TABLE 9: The Barrier of the Hydrogen Exchange Reaction

method	$E(H_3)$ (au)	$E(H_2+H)$ (au)	barrier (kcal/mol)
VBSCF	−1.61804	−1.65081	20.6
VBPT2	−1.65175	−1.66885	10.7
L-BOVB	−1.63485	−1.65115	10.2
VBCISD	−1.65655	−1.67246	10.0
CCSD(T)	−1.65689	−1.67246	9.8

10.7 kcal/mol is quite close to the VBCISD barrier (10.0 kcal/mol), itself within 0.2 kcal/mol of the reference CCSD(T) value.

3.7. Size Consistency. Size consistency is a key property for any modern computational method. Obviously, we are also concerned about the problem in the VBPT2 method. The size-consistency of the VBPT2 method was tested on the O_2, N_2 and F_2 diatomic molecules. To that aim, the energy of the separate atoms was, in each case, compared to the energy of the supersystem constituted of the two atoms separated by a long distance, 50 or 100 Å. Any important difference between the so-calculated energies would be the sign of a lack of size-consistency. The results, shown in Table 10, show that, in all cases, the energies of the supersystems are equivalent to the energies of the corresponding separate atoms, within 10^{-2} mhartree in all three cases, indicating an excellent size-consistency property of the VBPT2 method.

TABLE 10: VBPT2-Calculated Energies (hartrees) of Some Supersystems of Two Distant Atoms as Compared with the Summed Energies of the Separate Atoms

molecule[a]	$E(A_2)$	$2E(A)$	ΔE (size)
2N	−108.828718	−108.828718	$<0.1 \times 10^{-5}$
2O	−149.697247	−149.697240	0.7×10^{-5}
2F	−199.199010	−199.199003	0.7×10^{-5}

[a] $R_{NN} = 50$ a$_0$, $R_{OO} = 100$ a$_0$, $R_{FF} = 100$ Å.

4. Conclusions

This paper introduces the valence bond second-order perturbation theory (VBPT2) method, which uses a perturbation technique to improve the energetics after a VBSCF calculation. In the VBPT2 method, the reference wave function is flexibly defined, depending on the purpose of application, which can be a compact VBSCF wave function or even a VB wave function that includes a full structure set. From this point of view, VBPT2 has no limitation, in principle, since it can always be improved systematically by increasing the reference wave function. At the limit of a full VB set with delocalized orbitals, the VBPT2 method is identical to the MO-based CASPT2 method. By defining the first-order correction to VB function, the VBPT2 wave function is ultimately expressed in terms of a minimal number of fundamental structures that dictate the chemistry of the problem, as in the simple VBSCF method. In so doing, VBPT2 retains the simplicity of a classical VB presentation.

Compared to another post-VBSCF method, VBCI, the VBPT2 method is computationally efficient. No Hamiltonian matrix elements with nonorthogonal orbitals are required after the VBSCF step. Owing to the orthogonality between different orbital blocks, all matrix elements involved in the perturbation correction procedure of VBPT2 are easily computed by using the Condon−Slater rules. Roughly speaking, the computational cost of the perturbation step is approximately the same as in the traditional CASPT2 method.

The test calculations presented in this paper show that for the calculations of relative energies, such as bond energies, atomization energies, and reaction barriers, VBPT2 gives results that are at par with the VBCISD method, and match those of the MO-based MRCI and CASPT2 methods. For the total energy, VBPT2 values are always lower than those of VBCI with the same VBSCF wave function, indicating that VBPT2 covers more dynamic correlation than VBCI, since the excited structure space in VBPT2 is larger than that in the VBCI method. The total VBPT2 energies match those of CASPT2 if one uses a properly designed VB wave function as reference. To our knowledge, VBPT2 is the first VB method that provides total molecular energies that are comparable to those of MO-based methods for dynamic correlation.

As in other multireference perturbation methods, a contraction technique of the excited space, which is widely used in CASPT2,

could later be employed to further promote the computational efficiency of the VBPT2 method. This is under development.

Acknowledgment. The research in Xiamen is supported by the Natural Science Foundation of China (No 20533020, 20873106) and the National Basic Research Program of China (204CB719902). S.S. is supported by an ISF grant (16/06).

References and Notes

(1) See, for example: (a) Shaik, S., Hiberty, P. C. *A Chemist's Guide to Valence Bond Theory*; Wiley-Interscience: New York, 2007. (b) Weinhold, F., Landis, C. *Valency and Bonding*; Cambridge University Press: Cambridge, 2005. (c) Copper, D. L., Ed. *Valence Bond Theory*; Elsevier: Amsterdam, 2002. (d) Hiberty, P. C.; Shaik, S. *J. Comput. Chem.* **2007**, *28*, 137.

(2) McWeeny, R. *Int. J. Quantum Chem.* **1988**, *34*, 25.

(3) (a) Verbeek, J.; van Lenthe, J. H. *J. Mol. Struct. (THEOCHEM)* **1991**, *229*, 115. (b) van Lenthe, J. H. *Int. J. Quantum Chem.* **1991**, *40*, 201. (c) Balint-Kurti, G. G.; Benneyworth, P. R.; Davis, M. J.; Williams, I. H. *J. Phys. Chem.* **1992**, *96*, 4346.

(4) (a) Wu, W.; Mo. Y.; Cao, Z.; Zhang, Q. In *Valence Bond Theory*; Cooper, D. L., Ed.; Elsevier: Amsterdam, 2002; pp143−186. (b) Zhang, Q.; Li, X. *J. Mol. Struct.* **1989**, *189*, 413. (c) Li, J.; Wu, W. *Theor. Chim. Acta.* **1994**, *89*, 105. (d) Wu, W.; Wu, A.; Mo, Y.; Lin, M.; Zhang, Q. *Int. J. Quantum Chem.* **1998**, *67*, 287.

(5) (a) Goddard, W. A. *Phys. Rev.* **1967**, *157*, 81. (b) Ladner, R. C.; Goddard, W. A., III. *J. Chem. Phys.* **1969**, *51*, 1073.

(6) (a) Karadakov, P. B.; Gerratt, J.; Cooper, D. L.; Raimondi, M. *J. Chem. Phys.* **1992**, *97*, 7637. (b) Cooper, D. L.; Gerratt, J.; Raimondi, M.; Sironi, M.; Thorsteinsson, T. *Theor. Chim. Acta.* **1993**, *85*, 261. (c) Cooper, D. L.; Gerratt, J.; Raimondi, M. *Int. Rev. Phys. Chem.* **1988**, *7*, 59.

(7) (a) Hiberty, P. C.; Flament, J. P.; Noizet, E. *Chem. Phys. Lett.* **1992**, *189*, 259. (b) Hiberty, P. C.; Humbel, S.; van Lenthe, J. H.; Byrman, C. P. *J. Chem. Phys.* **1994**, *101*, 5969. (c) Hiberty, P. C.; Shaik, S. *Theor. Chem. Acc.* **2002**, *108*, 255.

(8) (a) Wu, W.; Song, L.; Cao, Z.; Zhang, Q.; Shaik, S. *J. Phys. Chem. A* **2002**, *106*, 2721. (b) Song, L.; Wu, W.; Zhang, Q.; Shaik, S. *J. Comput. Chem.* **2004**, *25*, 472.

(9) (a) Song, L.; Wu, W.; Hiberty, P. C.; Danovich, D.; Shaik, S. *Chem.—Eur. J.* **2003**, *9*, 4540. (b) Su, P.; Song, L.; Wu, W.; Hiberty, P. C.; Shaik, S. *J. Comput. Chem.* **2007**, *28*, 185. (c) Gu, J.; Lin, Y.; Ma, B.; Wu, W.; Shaik, S. *J. Chem. Theory Comput.* **2008**, *4*, 2101. (d) Su, P.; Wu, W.; Shaik, S.; Hiberty, P. C. *Chem. Phys. Chem.* **2008**, *9*, 1442.

(10) (a) Roos, B. O.; Linse, P.; Siegbahn, P. E. M.; Blomberg, M. R. A. *Chem. Phys.* **1982**, *66*, 197. (b) Andersson, K.; Maimqvist, P.-Å.; Roos, B. O.; Sadlej, J.; Wolinski, K. *J. Phys. Chem.* **1990**, *94*, 5483. (c) Andersson, K.; Maimqvist, P.-Å.; Roos, B. O. *J. Chem. Phys.* **1992**, *96*, 1218. (d) Andersson, K.; Roos, B. O. *Int. J. Quantum Chem.* **1992**, *96*, 591. (e) Ghigo, G.; Roos, B. O.; Maimqvist, P.-Å. *Chem. Phys. Lett.* **2004**, *396*, 142. (f) Azizi, Z.; Roos, B. O.; Veryazov, V. *Phys. Chem. Chem. Phys.* **2006**, *8*, 2727. (g) Aquilante, F.; Maimqvist, P.-Å.; Pedersen, T. B.; Ghosh, A.; Roos, B. O. *J. Chem. Theory Comput.* **2008**, *4*, 694.

(11) Wolinski, K.; Pulay, P. *J. Chem. Phys.* **1989**, *90*, 3647.

(12) (a) Hirao, K. *Chem. Phys. Lett.* **1992**, *190*, 374. (b) Hirao, K. *Chem. Phys. Lett.* **1992**, *196*, 397. (c) Hirao, K. *Chem. Phys. Lett.* **1993**, *201*, 59. (d) Kobayashi, Y.; Nakano, H.; Hirao, K. *Chem. Phys. Lett.* **2001**, *336*, 529. (e) Finley, J. P.; Hirao, K. *Chem. Phys. Lett.* **2000**, *328*, 51.

(13) (a) Werner, H.-J. *Mol. Phys.* **1996**, *89*, 645. (b) Celani, P.; Werner, H.-J. *J. Chem. Phys.* **2003**, *119*, 5044. (c) Celani, P.; Werner, H.-J. *J. Chem. Phys.* **2000**, *112*, 5546.

(14) (a) Murphy, R. B.; Messmer, R. P. *J. Chem. Phys.* **1992**, *97*, 4170. (b) Murphy, R. B.; Pollard, W. T. *J. Chem. Phys.* **1997**, *106*, 5073. (c) Sejpal, M.; Messmer, R. P. *Chem. Phys.* **2001**, *270*, 237. (d) Sejpal, M.; Messmer, R. P. *J. Chem. Phys.* **2001**, *114*, 4796.

(15) Dunietz, B. D.; Friesner, R. A. *J. Chem. Phys.* **2001**, *115*, 11052.

(16) Martinazzo, R.; Famulari, A.; Raimondi, M.; Bodo, E.; Gianturco, F. A. *J. Chem. Phys.* **2001**, *115*, 2917.

(17) Matsen, F. A. *Adv. Quantum Chem.* **1964**, *1*, 59.

(18) (a) Song, L.; Mo, Y.; Zhang, Q.; Wu, W. *J. Comput. Chem.* **2005**, *26*, 514. (b) Song, L.; Song, J.; Mo, Y.; Wu, W. *J. Comput. Chem.* **2009**, *30*, 399.

(19) Grein, F.; Chang, T. C. *Chem. Phys. Lett.* **1971**, *12*, 44.

(20) Lévy, B.; Berthier, G. *Int. J. Quantum Chem.* **1968**, *2*, 307; *Int. J. Quantum Chem.* **1969**, *3*, 247.

(21) (a) Shaik, S.; Shurki, A. *Angew. Chem., Int. Ed.* **1999**, *38*, 586–625. (b) Sharir-Ivry, A.; Crown, H. A.; Wu, W.; Shurki, A. *J. Phys. Chem. A* **2008**, *112*, 2489–2496.

(22) Frisch, M. J.; Trucks, G. W.; Schlegel, H. B.; Scuseria, G. E.; Robb, M. A.; Cheeseman, J. R.; Montgomery, J. A., Jr.; Vreven, T.; Kudin, K. N.; Burant, J. C.; Millam, J. M.; Iyengar, S. S.; Tomasi, J.; Barone, V.; Mennucci, B.; Cossi, M.; Scalmani, G.; Rega, N.; Petersson, G. A.; Nakatsuji, H.; Hada, M.; Ehara, M.; Toyota, K.; Fukuda, R.; Hasegawa, J.; Ishida, M.; Nakajima, T.; Honda, Y.; Kitao, O.; Nakai, H.; Klene, M.; Li, X.; Knox, J. E.; Hratchian, H. P.; Cross, J. B.; Adamo, C.; Jaramillo, J.; Gomperts, R.; Stratmann, R. E.; Yazyev, O.; Austin, A. J.; Cammi, R.; Pomelli, C.; Ochterski, J. W.; Ayala, P. Y.; Morokuma, K.; Voth, G. A.; Salvador, P.; Dannenberg, J. J.; Zakrzewski, V. G.; Dapprich, S.; Daniels, A. D.; Strain, M. C.; Farkas, O.; Malick, D. K.; Rabuck, A. D.; Raghavachari, K.; Foresman, J. B.; Ortiz, J. V.; Cui, Q.; Baboul, A. G.; Clifford, S.; Cioslowski, J.; Stefanov, B. B.; Liu, G.; Liashenko, A.; Piskorz, P.; Komaromi, I.; Martin, R. L.; Fox, D. J.; Keith, T.; Al-Laham, M. A.; Peng, C. Y.; Nanayakkara, A.; Challacombe, M.; Gill, P. M. W.; Johnson, B.; Chen, W.; Wong, M. W.; Gonzalez, C.; Pople, J. A. In *Gaussian 03*; Gaussian, Inc.: Wallingford, CT, 2004.

(23) Heitler, W.; London, F. *Z. Phys.* **1927**, *44*, 455.

(24) Heisenberg, W. *Z. Phys.* **1926**, *38*, 411.

(25) Bauschlicher, C. W., Jr.; Langhoff, S. R. *J. Chem. Phys.* **1987**, *86*, 5595.

(26) Rumer, G. *Göttingen Nachr.* **1932**, 337.

(27) Shaik, S.; Danovich, D.; Silvi, B.; Lauvergnat, D.; Hiberty, P. C. *Chem. Eur. J.* **2005**, *11*, 6358.

(28) Olsen, J.; Jorgensen, P.; Koch, H.; Balkova, A.; Bartlett, R. J. *J. Chem. Phys.* **1996**, *104*, 8007.

(29) Chase, M. W., Jr. *J. Phys. Chem. Ref. Data, Monogr.* **1998**, *9*, 1951; NIST-JANAF Thermochemical table, 4th ed.

(30) (a) Liu, B. *J. Chem. Phys.* **1973**, *58*, 1925. (b) Siegbahn, P.; Liu, B. *J. Chem. Phys.* **1978**, *68*, 2457. (c) Blomberg, M. R.; Liu, B. *J. Chem. Phys.* **1985**, *82*, 1050.

(31) Anderson, K.; Roos, B. O. *Int. J. Quantum Chem.* **1993**, *45*, 591.

(32) MOLPRO, version 2006.1, a package of ab initio programs: Werner, H.-J.; Knowles, P. J.; Lindh, R.; Manby, F. R.; Schütz, M.; Celani, P.; Korona, T.; Rauhut, G.; Amos, R. D.; Bernhardsson, A.; Berning, A.; Cooper, D. L.; Deegan, M. J. O.; Dobbyn, A. J.; Eckert, F.; Hampel, C.; Hetzer, G.; Lloyd, A. W.; McNicholas, S. J.; Meyer, W.; Mura, M. E.; Nicklass, A.; Palmieri, P.; Pitzer, R.; Schumann, U.; Stoll, H.; Stone, A. J.; Tarroni, R.; Thorsteinsson, T.

JP903011J